Sensorless Control of Surface Mounted PMSM and BDCM with New Starting Technique

Mona N. Eskander, and Osama M. Arafa
Dept. of Power Electronics
Electronics Research Institute
Cairo, Egypt

Osama A. Mahgoub
Dept. of Electrical Power and Machines
Faculty of Engineering, Cairo University
Giza, Egypt

Abstract - **In this paper, an accurate method for sensorless control of permanent magnet brushless motors is explained. The method doesn't include any modification to the classical construction of such motors and can be easily integrated within the drive electronics. It is applicable to both motor types, i.e. those with sinusoidal or trapezoidal back EMF.. The back EMF waveform is extracted on-line using simple algebraic expression through a newly proposed measurement setup. It is then used within the corrective phase of an extended Kalman filter (EKF). A method is proposed to detect rotor position at starting to enable maximum starting torque/ampere at the required direction of rotation. The method functionality is tested by simulation for both motor types. Simulation results show a good performance at very low speed.**

Keywords- **Synchronous motors, brushless DC motors, Kalmann filters, sensorless speed control**

I. INTRODUCTION

Permanent magnet brushless motors (PMBM) are widely used as a basic element in high performance servo drive systems due to its high efficiency and torque density. Two different types of PMBM are available; the sinusoidal back EMF type and the trapezoidal back EMF type. The first type is referred to as permanent magnet synchronous motor (PMSM) and the second type is referred to as brushless DC motor (BDCM). Recently, a lot of research has been focusing on the sensorless control of PMBM, which is an attractive solution to mechanical sensor problems, i.e. extra cost, wiring complexity, reduced reliability and demand for additional mounting space. Also space limitations, incompatibility with some harsh working environment and weight reduction considerations (e.g. aviation industry) represent the most apparent motives behind sensorless control research efforts. Sensorless control schemes for surface-mounted (SM) PMBM are mostly depending on direct or indirect back EMF detection since the other schemes employing inductance changes with rotor position are applicable only to interior magnet (IM) PMBM. Previous works [1-3] developed sensorless control schemes for BDCM based on direct EMF detection, where EMF zero crossings provide position and speed information six times the number of pole-pairs every rotor cycle. The major drawback of such technique is the availability of speed information once every one sixth of the electrical cycle which degrades the drive's dynamic performance.

Other authors [4-5] suggested a novel scheme for indirect back EMF detection functioning even at very low rotational speed. However, it involves some modification to the classical structure of such motors which is inconvenient since it requires a non-standard production of PMSM.

A comparative study dedicated to BDCM only have shown that substantial improvement in BDCM performance can be realized by adopting an extended Kalman filter (EKF) algorithm utilizing the open phase voltage measurement in its correction mechanism [6].

Silverio Bolognani, et al [7] introduced a high-performance sensorless PMSM drive based on EKF utilizing a motor model that includes electrical and mechanical system dynamics. The electrical system dynamics requires short filter cycle comparable to the electrical time constant, hence fast digital signal processing is a must. Also the 4x4 matrices due to the selected model further increases the hardware speed requirement.

In this study a unified and general approach for position and speed estimation capable of handling both SM PMSM and SM BDCM is introduced. The proposed technique is independent of the excitation current profile since PMSM can be excited using sinusoidal or rectangular current waveforms. A new formulation of EKF is proposed which deals only with mechanical system dynamics. The measurement model of the EKF is based on a newly proposed method for indirect back EMF detection. A method is proposed to detect rotor position at starting to enable maximum starting torque/ampere at the required direction of rotation. The theory of proposed scheme and simulation results of PMSM and BDCM are presented.

II. SM PMBM MODEL

The large air gap of SM PMBM helps maintain the magnetic circuit virtually free from saturation and keeping the winding's inductance nearly constant and independent of rotor position and excitation current. On the other hand, PMBMs used in servo applications never operate without current control loop, this further support our assumption regarding the linearity of magnetic circuit since we can enforce control rules that keep current within magnetic circuit's linearity limits. A quite general voltage equation of both surface-mounted PMBM motor types is:

978-1-4244-1676-9/08 /$25.00 ©2008 IEEE

$$\begin{bmatrix} v_a \\ v_b \\ v_c \end{bmatrix} = \begin{bmatrix} r_s & 0 & 0 \\ 0 & r_s & 0 \\ 0 & 0 & r_s \end{bmatrix} \begin{bmatrix} i_a \\ i_b \\ i_c \end{bmatrix} + \begin{bmatrix} L-M & 0 & 0 \\ 0 & L-M & 0 \\ 0 & 0 & L-M \end{bmatrix} \begin{bmatrix} pi_a \\ pi_b \\ pi_c \end{bmatrix} + \begin{bmatrix} e_a \\ e_b \\ e_c \end{bmatrix} \quad \text{.....(1)}$$

where: v_a, v_b, v_c : stator terminal voltage of phases a, b and c respectively (V).

i_a, i_b, i_c : currents of phases a, b and c (A)

p : differential operator.

L : self-inductance per phase (H).

M : mutual inductance between two phases(H)

e_a, e_b, e_c : back EMF of phases a, b & c (V)

r_s : stator resistance per phase (ohm).

Equation (1), which is valid under the condition of isolated neutral point, shows that the three motor phases seem as if they were three independent coils of equivalent inductance *(L-M)* (though in fact they mutually interact through the mutual inductance term). The three windings subject to the flux of a rotating magnet which induces a back EMF of value e_{ph} .

III. BACK EMF DETECTION

A Theory

Figure 1: External small inductor connected to each phase

In the circuit shown in Fig.1, let the circuit part from P to N represent one of these three independent coils, a small external coil is placed between points I (inverter's feeding point) and P (motor terminal). Writing the equations of voltage drop between points **P, N** and **i, P** respectively:

$$V_{PN} = R_{ph}.i + L_{ph}.di/dt + e \quad \text{.....(2)}$$

$$V_{ip} = R_x.i + L_x.di/dt \quad \text{.....(3)}$$

Where;

V_{pn} : voltage drop from **P** to **N**

V_{ip} : voltage drop from **P** to **I**

e : back EMF generated due to permanent magnet

L_{ph} : equivalent inductance (*L-M*) of the phase winding

R_{ph} : resistance (r_s) of the phase winding.

L_x,R_x : inductance and resistance of the external inductor r

i : phase current

Solving the two previous equations for e yields:

$$e = -\frac{L_{ph}}{L_x} V_{ip} + \left(\frac{R_x L_{ph}}{L_x} - R_{ph}\right) i + V_{PN} \quad \text{.....(4)}$$

The previous equation can be applied for each motor phase independently. For a total of 4 voltage measurements is needed since the EMFs of the three phases sum to zero. Regarding current measurement needed for equation (4), current control loop normally needs measurement of two phases' current, hence naturally provides the current measurement required by our proposed method.

B Conditions of validity

Equation (4) can be used on line to calculate the instantaneous value of the back EMF waveform to a reasonable degree of accuracy if the following presumptions could be satisfied.

i. The motor magnetic circuit is linear region, hence the inductance of the windings is fixed

ii. Inductive voltage drops across windings' inductance are too large compared with the resistive voltage drops

iii. Differential voltage measurement (and associated processing) at the selected points in Fig.1 is simultaneous and fast enough relative to the current control switching frequency.

iv. The external inductors are identical to each other with low-loss core, with constant inductance, minimum resistance and zero-mutual inductance These conditions can be met by careful design.

IV. SYSTEM STATE EQUATION

EKF requires a dynamic system model (a state equation) [13]. The state equation for our implementation will involve mechanical system dynamics with electromagnetic developed torque and load torque considered as deterministic system input. The state equation is written in continuous state-space form as follows:

$$\begin{bmatrix} \dot{\omega}_r \\ \dot{\theta}_r \end{bmatrix} = \begin{bmatrix} -\frac{B}{J} & 0 \\ 1 & 0 \end{bmatrix} \begin{bmatrix} \omega_r \\ \theta_r \end{bmatrix} + \begin{bmatrix} \frac{P}{2J} \\ 0 \end{bmatrix} (T_e - T_L) \quad \text{.....(5)}$$

where:

ω_r , θ_r : rotor's electrical speed position respectively.

B : Damping friction coefficient in N.m.s/rad.

J : Inertial of the rotating mass in N.m.s^2/rad.

P : Number of poles.

T_e , T_L : electromagnetic torque and load torque

The electromagnetic torque T_e is given by :

$$T_e = \lambda'_m \left(\frac{P}{2}\right)\left(\frac{3}{2} i_a \cos\theta_r + \frac{\sqrt{3}}{2}(i_b - i_c)\sin\theta_r\right) \quad \text{....(6)}$$

Discretization of equation (5) yields:

$$\begin{bmatrix} \omega_r(k+1) \\ \theta_r(k+1) \end{bmatrix} = \begin{bmatrix} e^{\frac{-T}{\tau}} & 0 \\ \tau\left(1 - e^{\frac{-T}{\tau}}\right) & 1 \end{bmatrix} \begin{bmatrix} \omega_r(k) \\ \theta_r(k) \end{bmatrix} + \quad (7)$$

$$\begin{bmatrix} \frac{P\tau}{2J}\left(e^{\frac{-T}{\tau}} - 1\right) \\ \frac{P}{2J}\left[\tau T + \tau^2\left(e^{\frac{-T}{\tau}} - 1\right)\right] \end{bmatrix} (T_e - T_L)$$

V. SYSTEM OUTPUT (MEASUREMENT) EQUATION

Consider the three-phase back EMF as measured system's output. This output z is in general given by a nonlinear equation of the form:

$$\mathbf{z}_k = h(\mathbf{x}_k, \mathbf{v}_k) \quad \text{.....(8)}$$

Where :

$\mathbf{z}_k$ Back EMF of the windings a,b & c detected at step k $\mathbf{x}_k$: State variables $[\omega_r(k) \quad \theta_r(k)]^T$.

$\mathbf{v}_k$: Random variable representing measurement noise.

For PMSM type, neglecting measurement noise term, the measurement equation $h(\mathbf{x}_k, \mathbf{v}_k)$ is given by:

$$\begin{bmatrix} e_a \\ e_b \\ e_c \end{bmatrix} = \lambda'_m \frac{d\theta_r}{dt} \begin{bmatrix} \cos\theta_r \\ \cos(\theta_r - \frac{2}{3}\pi) \\ \cos(\theta_r + \frac{2}{3}\pi) \end{bmatrix} \quad \text{.....(9)}$$

Where:

λ'_m :the permanent magnet flux in Wb linearizing equation (14). the Jacobean matrix H is :

$$\mathbf{H} = \lambda'_m \begin{bmatrix} \cos\theta_r & -\omega_r \sin\theta_r \\ \cos(\theta_r - \frac{2\pi}{3}) & -\omega_r \sin(\theta_r - \frac{2\pi}{3}) \\ \cos(\theta_r + \frac{2\pi}{3}) & -\omega_r \sin(\theta_r + \frac{2\pi}{3}) \end{bmatrix} \quad \text{.....(10)}$$

At each time step, the elements of **H** should be updated.

VI. EKF ESTIMATION CYCLE

EKF has an estimation cycle composed of two main phases, namely prediction phase and correction phase.

Prediction:Project the state ahead in time

$$\tilde{\mathbf{x}}_k = \mathbf{A}\hat{\mathbf{x}}_{k-1} + \mathbf{B}\mathbf{u}_{k-1} \quad \text{.....(11)}$$

$\tilde{\mathbf{x}}_k$: Prediction of the current state. $\hat{\mathbf{x}}_{k-1}$ Previous estimate of state, $\mathbf{u}_{k-1}$: system input

Project the state-prediction error covariance in time

$$\tilde{\mathbf{P}}_k = \mathbf{A}\hat{\mathbf{P}}_{k-1}\mathbf{A}^T + \mathbf{Q}_{k-1} \quad \text{.....(12)}$$

$\tilde{\mathbf{P}}_k$: prediction of covariance of state prediction error.

$\hat{\mathbf{P}}_{k-1}$: previous estimate of the covariance

$\hat{\mathbf{Q}}_{k-1}$: process noise covariance where process noise

Correction:Compute Kalman Gain

$$\mathbf{K}_k = \frac{\tilde{\mathbf{P}}_k \mathbf{H}_k^T}{\mathbf{R}_k + \mathbf{H}_k \tilde{\mathbf{P}}_k \mathbf{H}_k^T} \quad \text{.....(13)}$$

where, $\mathbf{R}_k$ is the measurement noise covariance.

Update estimate with measurement $\mathbf{Z}_k$

$$\hat{\mathbf{x}}_k = \tilde{\mathbf{x}}_k + \mathbf{K}_k(z_k - h(\tilde{\mathbf{x}}_k, 0)) \quad \text{.....(14)}$$

$\hat{\mathbf{x}}_k$: latest estimate of state (rotor speed).

z_k : the extracted back EMF as given by (4)

Update the state-prediction error covariance

$$\hat{\mathbf{P}}_k = (\mathbf{I} - \mathbf{K}_k \mathbf{H}_k)\tilde{\mathbf{P}}_k \quad \text{.....(15)}$$

VII. OPEN LOOP STARTING

The method proposed for rotor position detection at standstill depends on applying a step voltage to the field coil and monitoring the stator terminal voltage response due to it..

Dynamic motor equation is:

$$J P^2\theta_R + B.P\,\theta_R + T_L = \lambda_M I_S.SIN(\theta_S - \theta_R) \quad (16)$$

where i_s is stator current, θ_s angle w.r.t stator magnetic axis. At low speed, $\sin(\theta_S - \theta_R) \cong (\theta_S - \theta_R)$, H

$$\theta_{RC} = E^{-(B/2J)T}(C1 \sin\omega_N T + C2 \cos\omega_N T), \quad (17)$$

where, $\omega_n = \sqrt{(4J\lambda_m \mathbf{i_s} - B^2)} / (2J)$

For a smooth start, ramp speed command is imposed.

Dropping high frequency current ripples, gives θ_r

$\theta_r = \theta_{rc} + at^2/2 - aBt/\lambda_m \mathbf{i_s} + [(aB^2/\lambda_m \mathbf{i_s}) - 0.5\ a.J] / \lambda_m \mathbf{i_s}$

Differentiating θ_r to get rotor speed ω:

$$\omega = E^{(B/2J)T}[(-B/2J)C1 - \omega_N C2)SIN\ \omega_N T + (\omega_N C1 - (B/2J)$$

$$COS\ \omega_N T] + A.T - (AB/\lambda_M I_S)$$

where, a is acceleration.

For initial conditions $\theta_r = \theta_{r0}$ and ω=0, steady state component of speed response is $\omega_{ss} = a.t - (a.B / \lambda_m i_s)$

In Fig.2, without transient component,the motor speed follows the ramp command with an offset of $(a.B / \lambda_m i_s)$, which with small a, starting has minimum oscillation

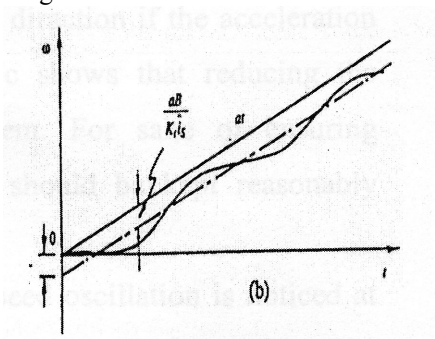

b) Minimum Oscillation

Figure 2. Minimum Starting oscillation

The results in Fig.3 for fan load applied to the BDCM at a=50 rad/s. show ω, θ and Te along the open loop period planned to accelerate motor to 20% of rated speed

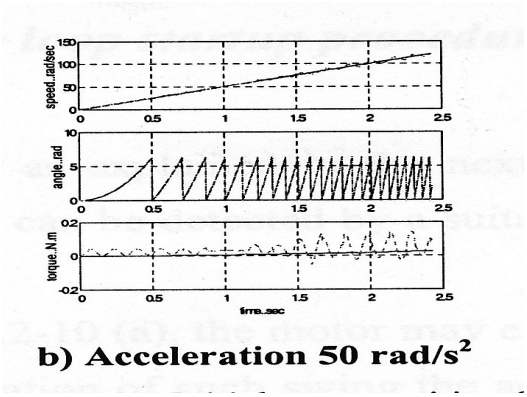

Figure 3. Open Loop Starting at $\theta_o = 0^o$

The rotor position detected has a maximum error of $\pm 30^o$ electrical, which is sufficient to determine the proper initial commutation sequence and to start accelerating the motor in the desired direction

VIII. SIMULATION

Fig.4 illustrates the flowchart of the PMBM simulation program written in MATLAB/SIMULINK environment. The particular type of the motor and of the applied excitation is informed to the program through an identification parameter to distinguish between two different running modes of the program; PMSM with sinusoidal type excitation and BDCM (trapezoidal type).

In block **3**, the speed error fed to that block from the comparison of speed command and the EKF estimated speed is being processed by a PI controller whose parameters are fed to the program in block **1**. This process results in torque command, which is then used to calculate the peak amplitude of current command. A formatting envelope with unity amplitude giving the waveform of the excitation current, according to running mode, is generated in block **9** based on EKF rotor position estimation. This envelope is used to issue the current command by direct amplitude modulation that takes place in block **4.**

PI current control then issues the voltage command to the inverter. Inverter control defines the inverter devices' status and hence the inverter/motor circuit topology. The proper set of differential equation is then picked up as in block **7** to calculate the current derivatives.

Numerical integration with reasonable fixed step size is then applied to the state derivatives to obtain current values (ω and θ are also obtained at this stage for comparison with EKF estimation results). Now motor currents are fed into block **8** where developed torque can be calculated and EKF is applied (Load torque is considered as disturbance). Speed and position estimation results from EKF are then used for closing the speed feedback loop and for creating excitation current template as per block **9.**

In the following figures the results obtained from simulation runs intended for testing the dynamic and steady state performance of the newly proposed method using this program and applied on a PMSM motor and a BDCM motor are presented. In these simulation runs, the speed profile shown in Fig.5 is applied. A no-load startup is initially allowed with a speed command of half the rated speed, and with zero initial rotor position. Then at t=0.1333 the full load torque is applied and speed command is suddenly raised to full rated speed. Motor successfully accelerates to the full rated speed in a forward direction as commanded.

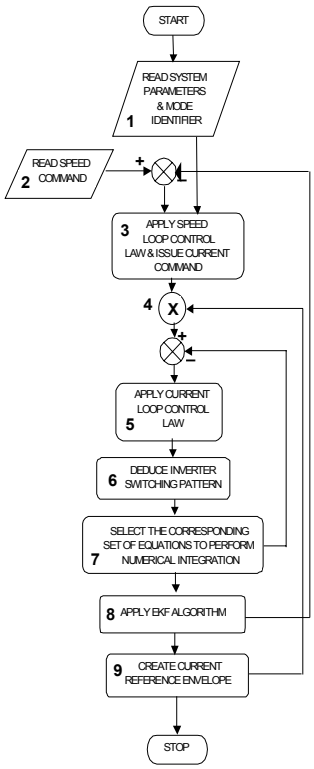

Figure 4 . Simulation program flowchart

At t=0.2666, the speed command is reversed and load torque is suddenly applied in the reverse direction. The motor decelerates to zero then accelerates in the reverse direction until rated speed is reached. Fig.6a illustrates the EMF detected by the proposed method for the PMSM with sinusoidal excitation. Its 3 phase current waveforms are shown in Fig.6b. The developed torque diagrams in Fig 6c show the acceleration periods where the torque value is within the limit imposed by the torque and current controllers until reaching the desired speed then drops off to the level required for load driving. Fig.7a through Fig.5c illustrates the same responses for a BDCM with trapezoidal excitation. The accurate estimation of rotor position is shown in Fig.8.

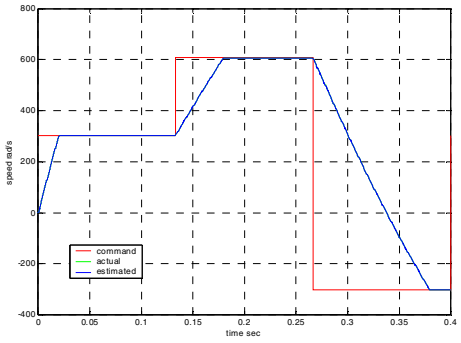

Figure 5. Motor speed profile

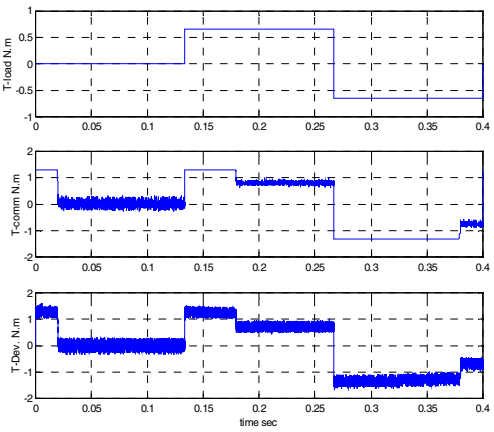

Figure 6c. PMSM Motor torque profile (Load/Command/Developed)

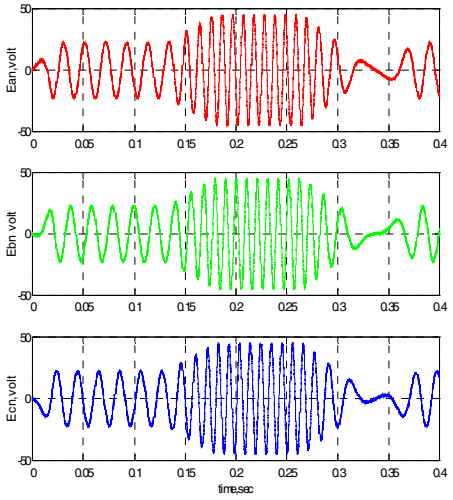

Figure 6a. PMSM EMF detected by the proposed method

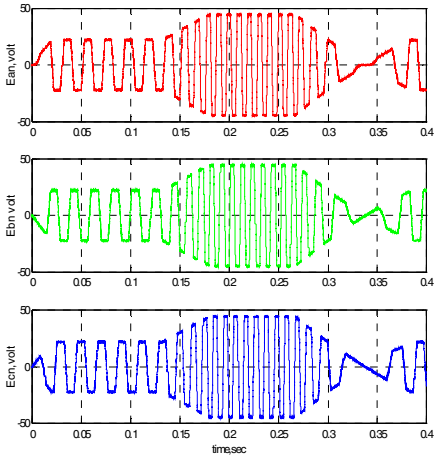

Figure 7a. BDCM EMF detected by the proposed method

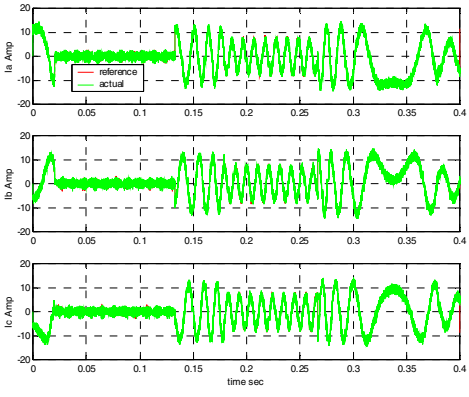

Figure 6b. PMSM Rotor current Waveforms

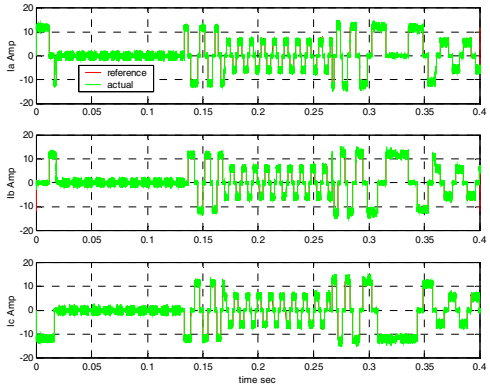

Figure 7b. Rotor Current Waveforms (phase A/B/C)

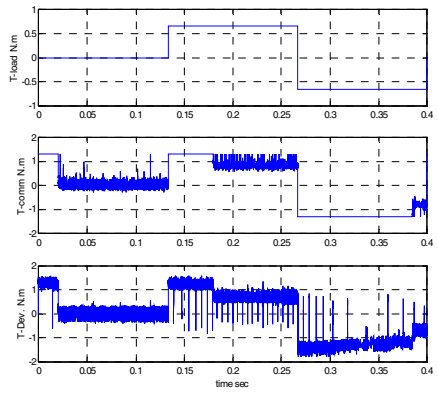

Figure 7c. BDCM Motor torque profile

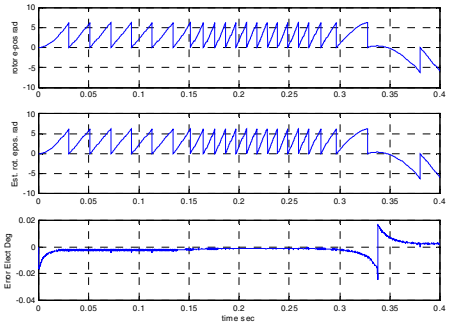

Figure 8. Electrical Rotor Position

VIII. CONCLUSION

A unified approach for PMBM sensorless speed control is proposed. The proposed controller is capable of providing superior control for both PMSM and BDCM. Three external coils are employed without extra taps or modifications in motor windings or construction.

Using a state model based on mechanical system dynamics with its virtually large time constant, allowing longer filter cycle, effectively reduces the intensive on-line arithmetic characterizing EKF. It also allows for reduced-size matrix manipulation (mostly 2x2 matrices) and thus further reduces the hardware speed requirement. This finally reduces the cost while still offering the high performance. The only drawback is the extra voltage amount that should be supplied by the inverter to compensate for voltage drop across the external inductors. Selecting inductors of proper values can minimize this drawback. Very small inductor value would result in low measurement accuracy. A compromise between reducing additional voltage and suitable measurement accuracy is accomplished using a value of 10% of motor inductance for the external inductor.

An open loop method is proposed to detect rotor position at starting to enable starting at the required direction of rotation. This method allows an error of only half oscillation in motor speed.

IX.APPENDIX

The parameters of a 2 pole, 400-watt SM PMSM motor are:

R (Resistance per phase)	=0.560	Ω
$L'=L_s-L_M$	=5.945e-4	H
λ'_m (Back EMF const)	=0.073	V/rad/s.
J (Inertia)	=831e-7	Kgm2
Rated Speed	=5800	R.P.M.

REFERENCES

[1] L. Cardoletti,A. Cassat,M. Jufer,,"Sensorless Position and Speed Control of a Brushless DC Motor from Start-up to Nominal Speed" ,EPE Journal, Vol.2, No.1 (1990), pp 25-34.

[2] D.M.Erdman, H.B.Harms, J.L.Oldenkamp, "Electronically Commutated DC motors for the Appliance Industry", IEEE-IAS Conf. Rec., Oct. 1984, pp 1339-1345.

[3] N. A. Demerdash, T. W. Nehl, E. Maslowski, "Dynamic modeling of brushless dc motors in electric propulsion and electromechanical actuation by digital techniques", IEEE IAC Conference , 1980, pp 570-579.

[5] S.Deepak , H. A. Toliyat, T. A. Nondahl, "Position Sensorless Control of Surface Mount Permanent Magnet AC (PMAC) Motors at Low Speeds", Proceeding of the American Control Conf. SanDiego, California, June 1999, pp 2141-2142.

[6] K. Rahman, H. A. Toliyat, "Sensorless Operation of Permanent Magnet AC motors with Modified Stator Windings", Industry Application. Conf., 31st Annual IAS Meeting, 1996, vol.1, pp 326-333.

[7] P Kettle, A Murray, F Moynihan, "Sensorless Control of a Brushless DC Motor using an Extended Kalman Estimator", PCIM'98 Intelligent Motion.Nurenberg, May 1998, Proceedings, pp 385-392

[8] S.Blognanai, M Zigliotto, M Zordan, "Extended-Range PMSM Sensorless Speed Drive Based on Stochastic Filtering", IEEE Transactions on Power Electronics, Vol.16, No.1, January 2001,pp110-116.